

Source substitution method for obtaining the power transmission from vibrating sources in buildings

Christoph Höller^{a,b,*}, Barry M. Gibbs^a

^a*Acoustics Research Unit, School of Architecture, University of Liverpool, L69 7ZN, Liverpool, United Kingdom*

^b*National Research Council Canada, Ottawa, Ontario, K1A 0R6, Canada*

Abstract

This paper describes a method analogous to the airborne sound source substitution method, to estimate the vibrational power injected by a structure-borne sound source into the supporting building element. The injected vibrational power is required for prediction of the structure-borne sound pressure from vibrating equipment in buildings. The paper focuses on high-mobility sources connected to low-mobility receivers, a situation which is commonly encountered in heavyweight construction. The mobility mismatch simplifies the transformation of laboratory measurement data to prediction of transmitted power in-situ. Three case studies were performed. In the first study, the power injected by a simple test source into a resiliently supported aluminium plate was determined using direct and indirect methods. Source substitution was investigated with different calibration options: steady-state excitation, transient excitation, and spatial averaging. The source power could be determined within 4 dB, compared with direct measurements of the injected power. In the second study, the power injected by a second source into a concrete transmission suite floor was determined. The third study was of a combined heating and power unit on a masonry wall. In this study, a reference sound pressure level in a receiver room was calculated and compared with a criterion curve for the assessment of low-frequency noise complaints. The case studies demonstrate that structure-borne sound source substitution is a promising development of the reception plate method. While the latter can be used if a free reception plate is available, the former circumvents problems of determining the transmitted power into coupled plates and therefore has application to real building conditions. The use of the instrumented hammer for the calibration and the use of spatial averaging significantly simplify the method.

Keywords: source power, indirect methods, structure-borne sound sources, building acoustics, measurement techniques, reception plate, substitution method

1. Introduction

The most important quantity for the calculation of structure-borne sound from vibrating sources into buildings is the power transmitted into supporting and other connected building elements [1, 2]. The transmitted power provides the input into energy-based prediction models, such as Statistical Energy Analysis [3, 4] or standardized procedures based on it [5], used for the prediction of sound pressure levels in buildings due to service equipment. For airborne sound power, there is a range

of national and international standards using different measurement methods [6]: from sound pressure in reverberation chambers [7, 8] or anechoic chambers [9, 10]; by intensity methods [11, 12], and by source substitution [13, 14]. This paper describes a method analogous to the airborne source substitution method, and discusses its advantages and disadvantages. It focuses on high-mobility sources connected to low-mobility receivers, a situation which is common in heavyweight buildings. The mobility mismatch allows the assumption that the source behaves similarly on different receiver structures and simplifies the transformation of laboratory measurement data to prediction of transmitted power in-situ. This paper also considers lab-

*Corresponding author

Email address: christoph.hoeller@nrc.ca (Christoph Höller)

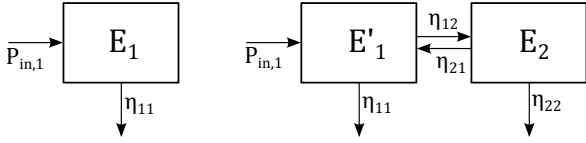


Figure 1: SEA model of an isolated reception plate, left, and of two connected plates, right.

oratory methods using isolated reception plates, for comparison with the source substitution method.

2. Isolated reception plates

A vibrating device, connected to an isolated (i.e. resiliently supported) reception plate, transmits power into the plate. When a steady state is reached, the transmitted power from the source into the reception plate is equal to the energy loss of the plate [15]. By plate energy is meant that determined by the bending wave field; other components of vibration are assumed secondary. Figure 1, left, illustrates the Statistical Energy Analysis (SEA) model of the process. Since the isolated reception plate is not connected to any other structures, there is only one subsystem in the model.

The power injected into the plate of area A and mass per area m'' can be calculated as:

$$P_{in,1} = \omega \eta_{11} m'' A \langle v^2 \rangle. \quad (1)$$

The frequency variable ω in Equation 1 indicates that the power injected into the plate is generally frequency-dependent. In an SEA framework, calculation and results are often captured in one-third octave band levels. The mean square velocity $\langle v^2 \rangle$ in Equation 1 is approximated by sampling the bending velocity field on the plate. The total loss factor η_{11} can be estimated from the structural reverberation time T_s [16]:

$$\eta \approx \frac{2.2}{f T_s}. \quad (2)$$

To minimise errors due to dominant plate eigenmodes, a minimum number of modes per frequency band is recommended, e.g. five or more modes in the frequency band of interest. An alternative indicator is the modal density (the number of modes per Hertz). The asymptotic modal density n_∞ of a thin plate of bending stiffness B is [16]

$$n_\infty = \frac{\Delta N}{\Delta f} = \frac{A}{2} \sqrt{\frac{m''}{B}}. \quad (3)$$

Modal density should be considered with total loss factor. If the total loss factor is low, the individual modes have a high Q factor and do not overlap sufficiently. A more appropriate measure is the modal overlap factor M , which is the ratio of the half-power bandwidth to the average frequency spacing between eigenfrequencies. For plate-like structures in buildings, Hopkins suggests a modal overlap factor of unity [16] as a lower limit for applying SEA. The modal density can be increased by increasing the plate area A and reducing the thickness h . An increase of the plate area has practical limitations. Reducing the thickness causes an unwanted increase in the plate mobility. Reference is made to the infinite plate mobility [15]:

$$Y_\infty = \frac{1}{8\sqrt{Bm''}}. \quad (4)$$

The infinite plate mobility is the mobility of a plate of the same properties as the actual plate but of infinite extent. It is real-valued and frequency-invariant. The asymptotic values in Equations 3 and 4 are simply related as

$$Y_\infty = \frac{n_\infty}{4Am''}. \quad (5)$$

Therefore, the requirement for a low mobility plate with a high modal density conflict.

A further challenge for the determination of the mean square velocity concerns the distribution of the plate bending energy. A large proportion of the energy of a free plate is stored along the edges and in the corners, especially at low frequencies. This is equivalent to the increase in sound pressure level at the walls and in the corners of reverberation chambers. For airborne sound sources, the Waterhouse [17] correction compensates for this systematic variation. For reception plates, Vogel et al. consider the edge effect, to find an equivalent correction factor [18, 19]. Since the plate velocity is measured at only a limited number of response positions, the selection of appropriate positions assumes importance. Späh and Gibbs investigate appropriate sampling strategies [20].

The total loss factor of the reception plate can be determined by measuring the structural reverberation time – the procedure is similar to that for measuring the reverberation time in rooms, but the energy decays are generally shorter. On an isolated plate, the total loss factor equals the internal loss factor, as the coupling losses and radiation losses are assumed negligible. The energy decay curve has

a single gradient and estimation of the loss factor is straightforward.

3. Connected reception plates

If the reception plate is connected to other plates, such as floors bonded into walls, part of the injected source power is lost to the other plates. Figure 1, right, illustrates a reception plate with a single connected plate as a SEA model with two subsystems. The power balance equations of the coupled plate system as shown in Figure 1 are

$$P_{in,1} = \omega\eta_{11}E_1' + \omega\eta_{12}E_1' - \omega\eta_{21}E_2 \quad (6)$$

$$0 = \omega\eta_{22}E_2 + \omega\eta_{21}E_2 - \omega\eta_{12}E_1'. \quad (7)$$

The first terms on the right-hand side in Equations 6 and 7 describe the internal losses. The second terms describes the energy lost to the other subsystem. The third term represents the power returning from the other subsystem. For a visual representation of these power flows, see Figure 1. To obtain the injected source power, the energy in both subsystems must be known as well as the internal loss factor and the coupling loss factors. Using only the internal loss factor and energy of subsystem 1 will give an incorrect estimate of the transmitted source power. Hopkins and Robinson [21] found that vibration levels can increase, due to returning energy from connected building elements. A typical energy decay curve of a free plate measurement is a straight line with a single gradient (on a log-linear scale). For a connected element, the energy decay curve typically shows a changing gradient. Figure 2 shows the idealized energy decay curves of a free plate and of the same plate connected to a second plate, calculated using Transient SEA [21].

Single gradient fits of such energy decay curves result in an over-estimate of the structural reverberation time and consequently in an under-estimate of the loss factor and the source power. However, when combined with the overestimate of energy, due to the returning energy component, Hopkins and Robinson show that the two effects can partly compensate each other, but this depends on the building situation.

A further complication is in estimating the mass of real building elements, where it is not obvious how much of the support structure should be included. In addition, real building elements may have a composite nature. The modal behaviour of coupled plates differs from that of free plates

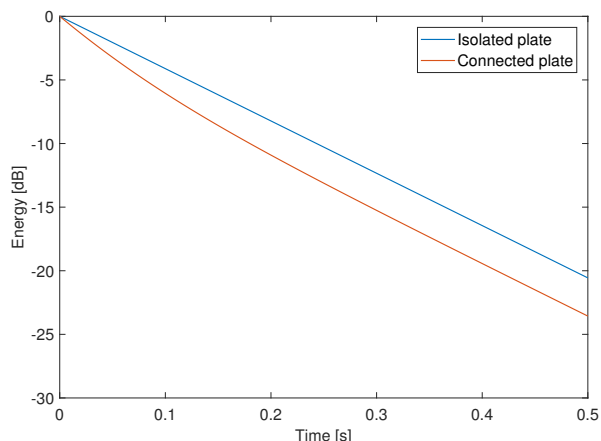


Figure 2: Idealized energy decay curves for isolated and connected plate.

and the sampling strategy therefore must be modified. Using connected walls and floors as reception plates can incur significant errors and alternative approaches are required.

4. Source substitution method

In seeking an alternative test method to determine structure-borne source power, reference is made to methods for the measurement of airborne source power. The airborne sound power level can be determined by employing a standardized source with known power into the room, and measuring the resulting sound pressure levels at fixed positions [13, 14]. The standardized source then is replaced by the source of interest, and the sound pressure levels measured again at the same positions. Assuming that the ratio between source power and sound pressure squared does not change, the source power can readily be calculated.

Unlike for airborne sources, the transmitted power of vibrating sources generally depends on both source and receiver mobilities [1, 2]. Therefore, a standardized source with known power output is not feasible. However, useful approximations are possible when the receiver mobility is much lower than the source mobility. Larsson and Simmons [22] employed the standard tapping machine as a reference source. The machine of interest is placed on the floor and the average velocity on the floor recorded during operation. Alternatively, the average sound pressure level in a receiving room can be measured. The machine is then replaced by the standard tapping machine and the average velocity

on the receiver plate (or the average sound pressure level) is recorded again, at the same positions. The velocity level difference (or sound pressure level difference) is calculated. The method uses the standard tapping machine and provides an “equivalent force” that can be used in prediction models [23]. A disadvantage is that sources attached to walls cannot be measured, as the standard tapping machine cannot be operated in a vertical position. Scheck overcame this by using an electro-dynamic device with the same force spectrum as the standard tapping machine [24].

The approach described in this paper makes use of the fact that the emitted power of a reference source can be measured directly by recording the force and velocity at the contact locations: $L_{W,cal} = 10 \log_{10}(\Re \{v_c F_c^*\})$. The measurement procedure is in two stages. A known power is injected into the receiver plate by a shaker at the anticipated source location and with the source not in place. The resulting response velocities due to the injected power are sampled over the plate. The shaker is then replaced by the source of interest, and the velocities are re-measured at the same response positions. The source power is obtained from these quantities.

4.1. Calibration sources

An electro-mechanic shaker provides control of the excitation spectrum and level for a good signal-to-noise ratio. However, the shaker can pose practical difficulties, especially when conducting measurements in the field. Suspending a sometimes heavy shaker and fixing it to a wall without inducing moments can be problematical and time-consuming. An instrumented impulse hammer provides an alternative. The hammer is easily moved to different excitation positions. However, control of the excitation level depends on operator skill and on the choice of hammer tips. The transient excitation signal complicates signal processing. Important questions remain. First, is the ratio of transient velocity response to transient power input the same as for the steady-state case? Secondly, would a single power calibration for the floor or wall be applicable for all sources at all locations? To investigate these and other questions, both steady-state excitation with a shaker and transient excitation with an instrumented hammer were investigated, and an average power calibration for the entire receiver was considered.

4.2. Averaging considerations

Most structure-borne sound sources have multiple connection points with the receiver structure. The “calibrated” input power $L_{W,cal,i}$ and the response velocities $L_{v,cal,i,j}$ at j remote positions have to be measured for each source contact i . For practical purposes, the averages $L_{W,cal}$ and $L_{v,cal,j}$ can be used for the calculation of the total source power. At each contact point i , the operating source exerts forces and moments on the receiver structure. An electro-mechanic shaker only exerts a force perpendicular to the receiver structure. Like the reception plate method, the source substitution method yields a single equivalent value for the source power which incorporates both force and moment transmission.

The number of remote response positions j can be chosen as needed. Theoretically, the source substitution method requires only one response velocity. However, accelerometer positions may be close to nodal lines, and increasing the number of response positions reduces such effects. Also, response positions should be chosen far enough from the source to avoid nearfield effects.

Once the input power $L_{W,cal}$ and the velocity responses $L_{v,cal,j}$ and $L_{v,source,j}$ have been recorded, there are several ways of evaluating the data. Three procedures are distinguished: In the first option, the source power is determined from the input power and the averaged velocity responses:

$$L_{W,source} = L_{W,cal} - \overline{L_{v,cal}} + \overline{L_{v,source}} \quad (8)$$

$\overline{L_{v,cal}}$ and $\overline{L_{v,source}}$ are the velocity levels for the calibration source and the source under test, respectively, averaged over all j response positions. Equation 8 corresponds to the averaging procedure used in ISO 3743. The mean square velocity on the plate is calculated for the calibration and measurement stages each. This can be considered an energetical approach, as the mean square velocity is proportional to the energy on the plate. In fact, Equation 8 can be derived from the power balance equation that forms the basis of the reception plate method (Equation 1). A reasonably reverberant field is required, and response positions close to the source have a larger influence on the result than response positions further away. The term $L_{W,cal} - \overline{L_{v,cal}}$ is termed the *power calibration term* in the following.

In option 2, the source power is determined from the average difference between the injected calibration power and the resulting velocity responses.

This option resembles a transfer function approach, rather than an energetical approach:

$$L_{W,source} = \overline{L_{v,source}} + \overline{L_{W,cal}} - \overline{L_{v,cal}} \quad (9)$$

The level differences $L_{W,cal} - L_{v,cal,j}$ are averaged and added to the mean square velocity level during operation of the source.

Finally, option 3 comes closest to the ideal of a substitution method:

$$L_{W,source} = L_{W,cal} + \overline{L_{v,source}} - \overline{L_{v,cal}} \quad (10)$$

The differences in velocity level between calibration stage and measurement stage are calculated for each individual response position j . The average velocity level difference $\overline{L_{v,source}} - \overline{L_{v,cal}}$ is calculated. This results in a constant “weighting” of the accelerometer positions, and possibly in a smaller standard deviation. The term $\overline{L_{v,source}} - \overline{L_{v,cal}}$ is referred to as *velocity level difference*.

For the case studies, options 1 and 3 were used. The power injected by a source into a receiver structure depends on the mobilities of both source and receiver, when they are of the same order. Therefore, the determination of source power is only useful if the installation during measurement resembles the final installation. This assumption is allowed for high-mobility source situations where $|Y_{source}| \gg |Y_{receiver}|$. The acquired source data then is transferable to other similar installations. If the source data does not have to be transferable, but is only required for the mounting situation at hand, the source substitution method applies even for source-receiver matched mobility conditions and also non-homogeneous receiver structures.

5. Case Study 1 – Test source on a free plate

In the first case study, the structure-borne power from a test source into an isolated plate was determined, using direct measurement, the reception plate method, and the source substitution method. The test source consisted of a fan base with the fan replaced by a top-mounted shaker (see Figure 3). The shaker was fed with pink noise for measurement over the frequency range of interest (20 Hz–2 kHz). This is the same test source and receiver plate that was used in a related study on the indirect determination of blocked forces [25].

The fan base incorporated force transducers at the support points and was rigidly glued to the

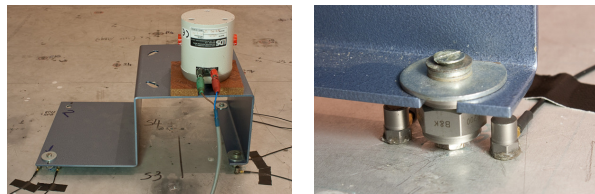


Figure 3: Setup for Case Study 1, showing force transducers and accelerometer pairs at the contacts between the test source and the free aluminium receiver plate.

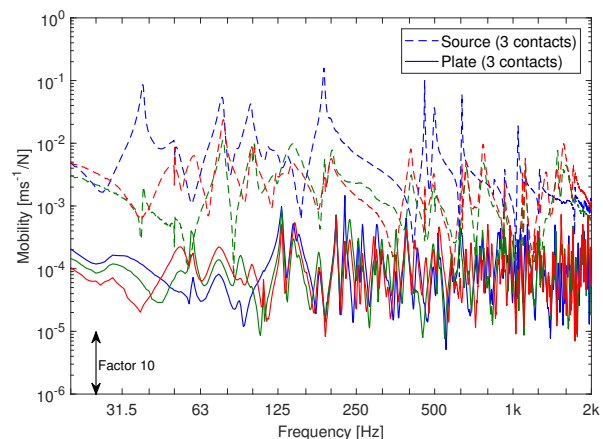


Figure 4: Case Study 1 – Narrowband source and receiver mobilities at the three contact points, measured according to ISO 7626 [26].

plate. Three of the four feet were connected to the plate to ensure a stable connection at the contacts. The coordinates of the three source contacts were (0.325 m, 0.38 m), (0.63 m, 0.38 m), and (0.63 m, 0.55 m).

The reception plate was of aluminium ($E = 70$ GPa, $\rho = 2700$ kg/m³, $\mu = 0.33$) of size 2.12 m \times 1.50 m \times 20 mm. It was supported at the corners and edges by visco-elastic pads. This setup approximates free (FFFF) boundary conditions. Source and receiver mobilities were measured directly according to ISO 7626 [26], and are shown in Figures 4 and 5. Generally, the source mobilities are an order of magnitude higher than the plate mobilities as indicated in the one-third octave band values. The narrowband mobilities reveal that the source mobility can occasionally be of the same order of magnitude as the receiver mobility. At these frequencies, peaks in transmission can occur [1, 2].

5.1. Source power by direct measurement

The power injected by the test source into the plate was obtained directly from the forces reg-

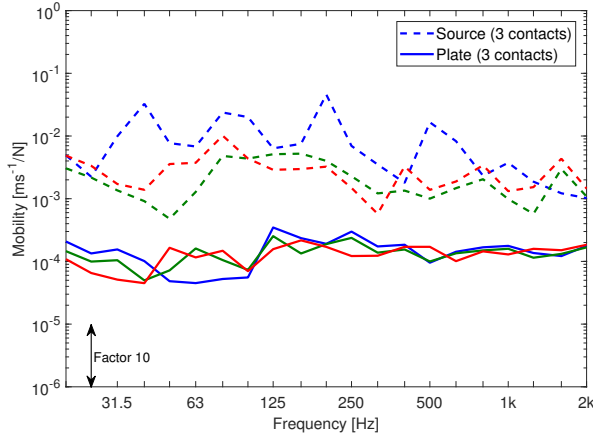


Figure 5: Case Study 1 – One-third octave band source and receiver mobilities at the three contact points, measured according to ISO 7262 [26].

istered at each mount transducer and velocities recorded by matched accelerometer pairs near each mount. The source power was calculated as

$$L_{W,source} = 10 \log_{10}(\Re\{v_1 F_1^* + v_2 F_2^* + v_3 F_3^*\}). \quad (11)$$

The calculation was performed with narrowband data, and the result transformed to one-third octave bands. The repeatability was obtained by repeating the measurement a second time without modifying the set-up, and the reproducibility was obtained by disassembling the set-up, reassembling and repeating the measurement once. The results are shown in Figure 6. The reproducibility exceeds the repeatability but is within 4 dB, though more repetitions would be necessary to establish reliable values for repeatability and reproducibility.

5.2. Source power by reception plate method

For the reception plate method, the total loss factor of the plate was determined using the decay method. The plate was excited by a shaker at the three source contact positions, and the decays measured at ten response positions. The average frequency-dependent structural reverberation time was calculated from the resulting 30 decay curves, and the total loss factor was determined from the average reverberation time.

The mean square velocity on the plate was measured in one-third octave bands (averaging time 30 s) at ten accelerometer positions. The source power in Figure 7 was calculated as in Equation 1. The repeatability and reproducibility of the measurement are shown in Figure 8.

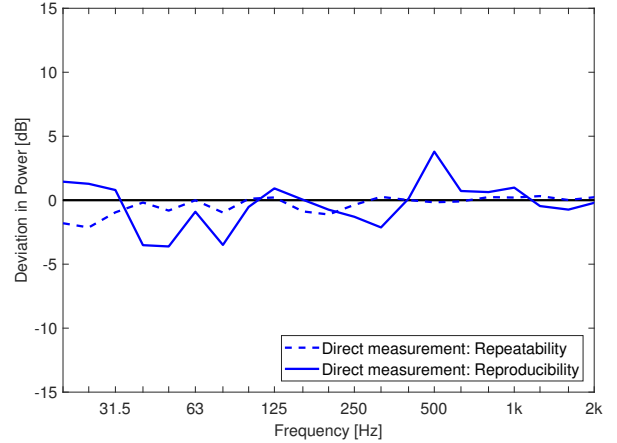


Figure 6: Case Study 1 – Direct measurement – Repeatability and reproducibility of the direct source power measurement.

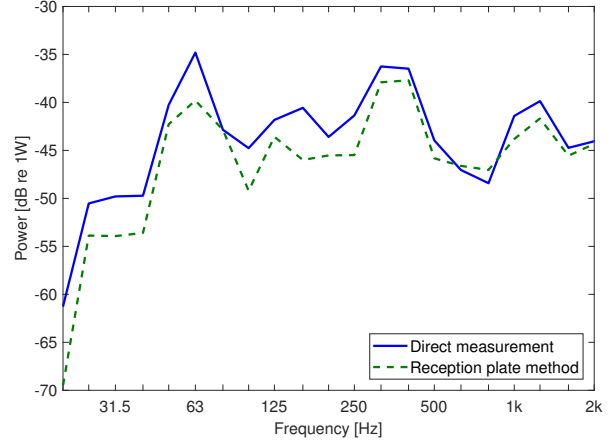


Figure 7: Case Study 1 – Reception plate method – Injected power from the test source into the free plate.

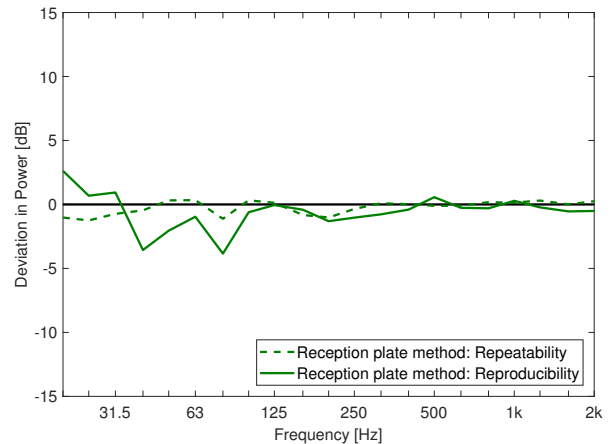


Figure 8: Case Study 1 – Reception plate method – Repeatability and reproducibility of the reception plate power measurement.

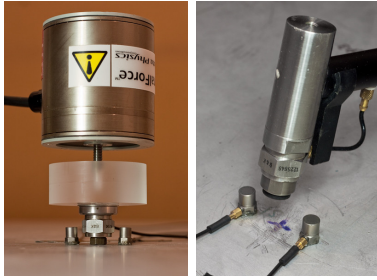


Figure 9: Case Study 1 – Plate calibration with shaker (left) and hammer (right).

The obtained source powers from direct measurement and from the reception plate method (see Figure 7) show the same trend, with the latter giving an under-estimate of up to 4 dB, which is similar in magnitude as the reproducibilities in Figures 6 and 8. This difference is likely due to small changes in the connection of the shaker to the metal base, in contact conditions between source and plate, in variations of the excitation signal, and in the accelerometer attachment conditions. The under-estimate can be explained by revisiting Equation 1. The plate mass can be estimated accurately and it can be assumed that the loss factor can be obtained with reasonable accuracy. However, the measured mean square velocity depends on careful choice of response positions [20, 27].

5.3. Source power by substitution method

The source power was determined using the substitution method, with three different configurations: using steady-state excitation, using transient excitation, and using spatial averages. The results are shown in Figure 13 and discussed in Section 5.4.

5.3.1. Source substitution using steady-state excitation

An inertial shaker (Figure 9, left) was used as a steady-state calibration source. The free aluminium plate was excited at the three source contacts and force and velocity at the contact were recorded. The input power was taken from the real part of the cross-spectrum. Simultaneously, the autospectra of the plate velocities squared at the same ten positions as for the reception plate method were recorded.

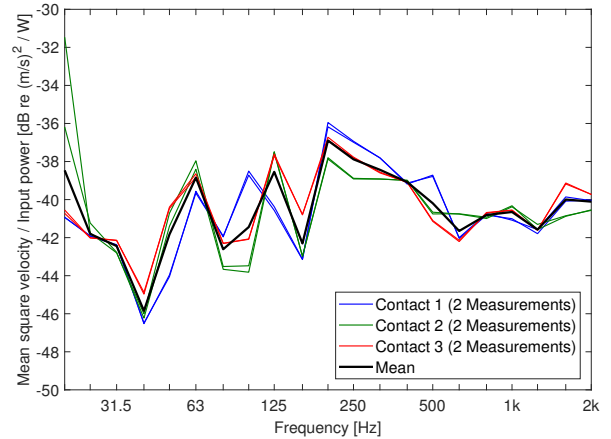


Figure 10: Case Study 1 – Source substitution method – Power calibration term for steady-state excitation with a shaker.

5.3.2. Source substitution using transient excitation

An instrumented hammer simplifies the measurement but increases the signal processing involved. The plate was excited with a hammer and in-line force transducer (Figure 9, right) at the three contact positions. Force and velocity at the contacts were recorded as time signals, then time-windowed (uniform window) and transformed to the frequency domain. The narrowband injected power is the real part of the product $\Re\{v_r F_r^*\}$. The narrowband power was then transformed to one-third octave band values. The same signal processing was applied to the recorded plate velocity time signals.

5.3.3. Source substitution using spatial averages

The substitution method was employed with the impulse hammer for transient calibration. This time the plate was excited at ten positions remote from the source contacts. The velocity responses were recorded at ten fixed response positions and an average calibration factor obtained, independent of impact position. The same signal processing applied and the same ten response positions were used.

5.4. Results and discussion

Figures 10, 11, and 12 show the power calibration terms $L_{W,cal} - \overline{L_{v,cal}}$ for the steady-state excitation, transient excitation, and spatial average, respectively. The mean values are indicated by the thick black line in each plot. For Figure 10, the range between the individual power calibration terms for

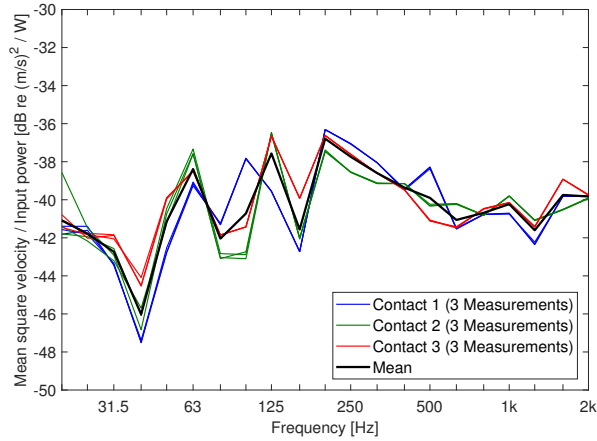


Figure 11: Case Study 1 – Source substitution method – Power calibration term for transient excitation with a hammer.

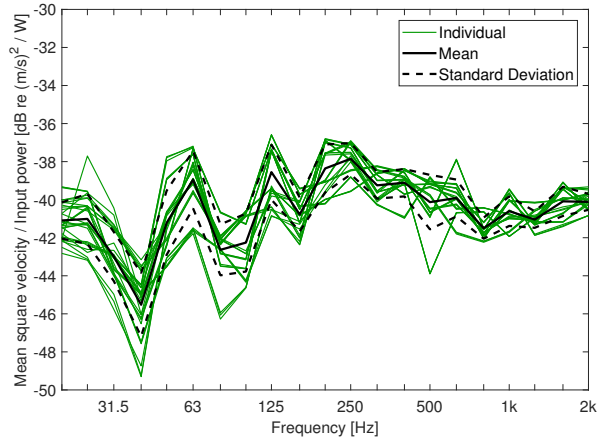


Figure 12: Case Study 1 – Source substitution method – Power calibration term for hammer excitation at 10 remote locations.

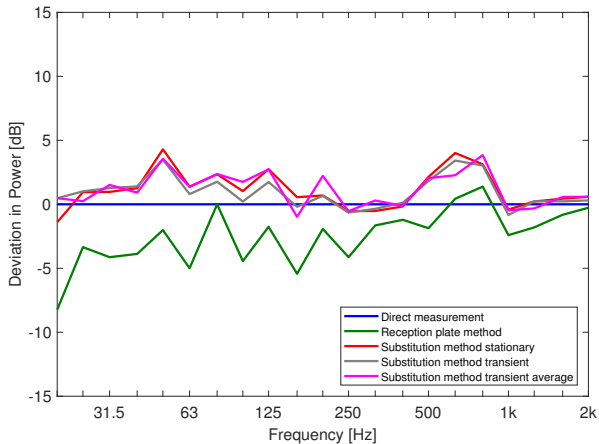


Figure 13: Case Study 1 – Source substitution method – Deviations in determined source power.

each of the three source contacts is 3 dB except at 20 Hz. For transient excitation in Figure 11, the results are similar to Figure 10. The power calibration terms in Figure 12 display a larger spread, but the mean value is again quite close to the mean value in the other plots. This also becomes apparent when comparing the calculated source power in Figure 13. In each case, the mean value was used for the source power calculations. The estimated powers are shown in Figure 13, normalised with respect to the direct measurement.

The source substitution results for steady-state excitation are the same, regardless of the averaging procedure. Option 1 can be used, which is less rigorous than option 3, using velocity level differences. Source substitution gives an average deviation in power of about 1 dB, with a maximum overestimate of 4 dB. The underestimate from the reception plate method is obtained from Figure 7.

The agreement between results for transient and stationary calibration are encouraging, and of practical benefit. The use of a hammer is much easier than of a shaker, particularly in the field. The three source substitution results agree within 1 dB. Again, the over-estimates compared with the directly measured power are within 4 dB. The spatial average calibration yields the source power with the same accuracy as with calibration terms at each source contact. With spatial average calibration, receiver structures can be calibrated once and then used for any source at any location.

6. Case Study 2 – Test source on a connected plate

In the second case study, a source previously used for a round robin (RR) survey [28] was used. The RR source was an aluminium plate of size $0.5 \text{ m} \times 0.35 \text{ m} \times 10 \text{ mm}$ on three mounts and was driven by a shaker, with pink noise as the excitation signal. A force transducer, between the shaker and the source plate, monitored and controlled the operating conditions. The concrete floor on a small transmission suite was used as receiver. It is of size $2.1 \text{ m} \times 3.1 \text{ m} \times 0.13 \text{ m}$, with an 8 mm epoxy mortar layer. Figures 14 and 15 show details of source and receiver.

The same five source positions were used as were prescribed for the round robin test [28]: near a corner, near an edge, in the middle, and two random positions. The design of the RR source prevented direct measurement of contact forces and thus the



Figure 14: The concrete floor of a small transmission suite was used as receiver structure for Case Study 2. The floor has dimensions of 2.1 m \times 3.1 m and is approximately 130 mm thick. It is supported by masonry walls on four sides and can therefore not be considered a “free” plate as required for the reception plate method.

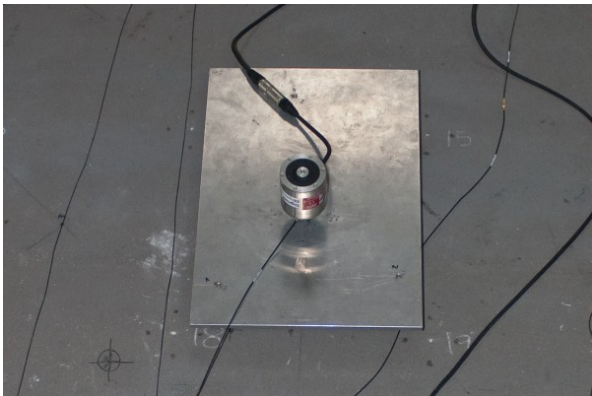


Figure 15: A test source originally developed for a round robin test of the reception plate method [28] was used for Case Study 2. The source consists of an aluminium plate which is excited by an attached shaker. Three feet transmit the vibrational energy to the receiver structure.

direct calculation of the injected power. Therefore, the previously measured RR source power, into a resiliently supported 100 mm concrete plate, obtained from the round robin test [28], was used for comparison.

6.1. Source power by reception plate method

Even though the reception plate method only applies for isolated plates, it was used here with a connected plate to show the potential deviations that the connected building elements introduce. The difficulties of using the adapted reception plate method with connected plates are: the boundary conditions of the floor are not well-defined; the mass of the floor is not known accurately due to the composite nature and uncertain dimensions of the floor; the railing presents an additional transmission path; loss factor measurements show that there is energy transfer into the supporting walls. It is for configurations like this that the source substitution method is proposed.

6.2. Source power by substitution method

6.2.1. Source substitution using steady-state excitation

The floor was calibrated with a large shaker with an in-line force transducer and matched accelerometer pairs, on either side of the force transducer.

The velocity responses at nine remote positions on the plate were simultaneously recorded for each of the five source locations. The shaker was placed at each of the three source contacts, for each of the five source locations, resulting in 15 measurements of $L_{W,cal}$ and $L_{v,cal}$. The source power was calculated for each source position, and the mean is used in the following for the comparisons.

6.2.2. Source substitution using transient excitation

The calibration of the concrete floor was repeated with the calibrated hammer. The same excitation and response positions were used for the determination of the power calibration term. Only the method of excitation was varied. Figure 16 shows the power calibration term, compared with steady-state values using the shaker. The agreement is within 3 dB over the frequency range of interest.

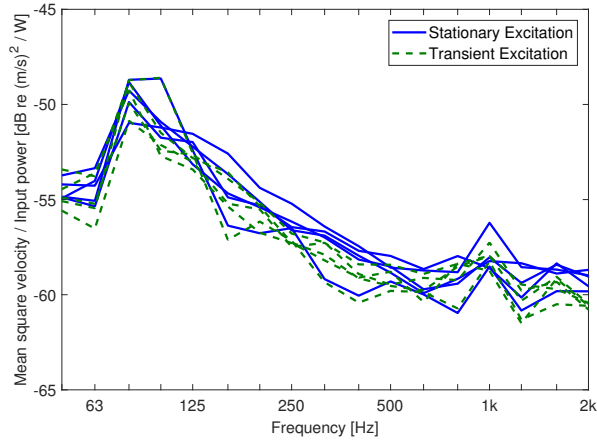


Figure 16: Case Study 2 – Source substitution method – Power calibration terms for shaker and hammer measurements.

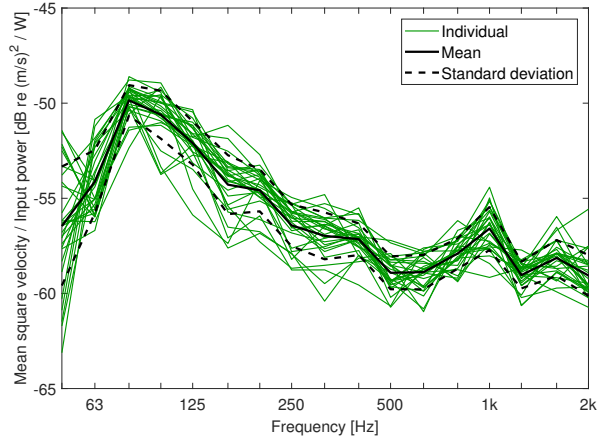


Figure 17: Case Study 2 – Source substitution method – Average power calibration term for 28 excitation positions and 9 fixed response positions, for the five source positions considered.

6.2.3. Source substitution using spatial averages

An average calibration factor was obtained for the floor of the transmission suite. The floor was excited by the large shaker at 28 locations. For each, the response velocities at nine fixed positions were recorded. Assuming a logarithmic normal distribution, the standard deviation, shown in Figure 17, is about 1 dB, for frequencies above 63 Hz.

6.3. Results and discussion

The power determined using the source substitution method with stationary calibration in Figure 18 fluctuates about the RR reception plate value within 6 dB, up to 1 kHz. The adapted re-

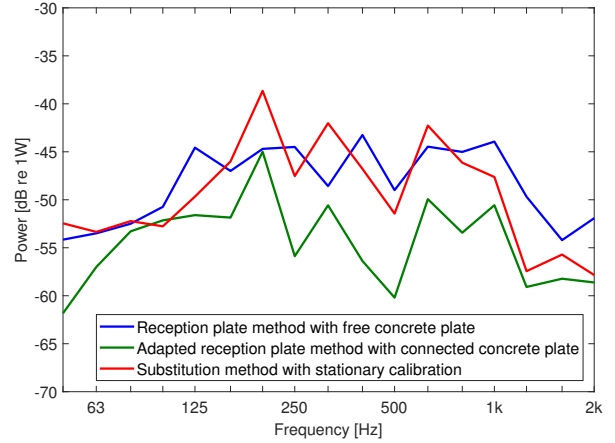


Figure 18: Case Study 2 – Source substitution method – Mean values of source power.

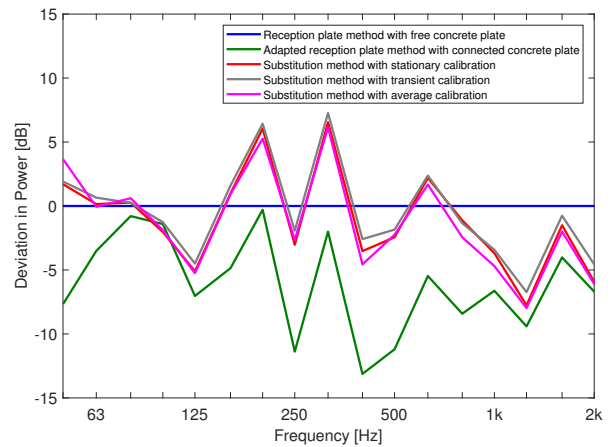


Figure 19: Case Study 2 – Source substitution method – Deviations in determined source power.

ception plate method with connected plates gives an under-estimate of up to 8 dB compared with the RR reception plate method.

Figure 19 shows the resultant RR source powers, presented as deviations from the RR reception plate value. The power determined by the source substitution method with transient calibration is in close agreement with the power from the steady-state calibration. The transient excitation gives 0.5 dB higher values on average than the steady-state value. The average calibration yields results within 0.2 dB of the steady-state calibration. Again, the hammer has practical advantages compared with the shaker, when measuring in this field-like situation. The adapted reception plate method with connected plates is clearly not appropriate for this situation.

7. Case Study 3 – Central heating and power unit on masonry wall

In the third case study, the source under test was a wall-mounted heating and power unit (“micro-CHP unit”). The internal excitation mechanisms generated both broadband and strong low-frequency tonal components. The micro-CHP unit was operated on a masonry wall of a reverberation chamber. The gas burner and other auxiliary devices were not operated. Instead, the unit was run in reverse: the engine was supplied with electricity and its operation cooled down the system. Direct measurement of the injected vibrational power was not possible, due to inaccessible contact points. However, the electrical power (voltage and current) to run the engine was monitored to ensure the same settings and operating conditions for all measurements. The source substitution method was employed to determine the injected vibration power. For practical reasons, only the instrumented hammer was used to determine the power calibration term.

7.1. Source power by substitution method

The unit was operated and the velocity response levels were recorded at ten remote response positions. Figure 20 shows the velocity signals on the wall during operation and background noise measurements. The excitation is dominated by tonal components at 50 Hz, 100 Hz, and 150 Hz. In the other frequency bands, the excitation does not exceed the background noise level.

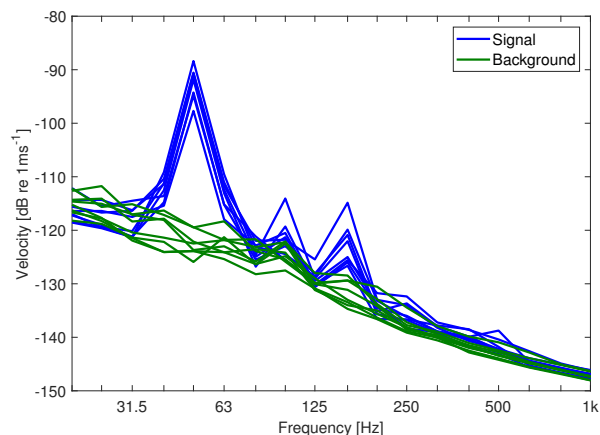


Figure 20: Case Study 3 – Velocities on the receiver wall.

7.1.1. Source substitution using transient excitation and spatial averages

A calibrated impulse hammer with a rubber tip was used for calibration. This allowed evaluation of the data up to 1 kHz. The receiver wall was excited at twelve positions and the input power and response velocities at ten remote response positions were recorded prior to the installation of the source.

7.1.2. Source substitution using transient excitation and spatial averages, with source mounted on the wall

The micro-CHP is an example of a source that is difficult to remove once installed. For such sources, the determination of the power calibration term with the source in place is of interest. This requires that the source mobility is much higher than the receiver mobility, so as to not dynamically load the receiver plate. For the micro-CHP unit, the measurements from Section 7.1.1 were repeated, but with the source mounted on the wall. Based on preliminary mobility measurements which showed that the source mobility was at least 10 dB higher than the receiver mobility for the entire frequency range of interest, it was expected that the power calibration term would not be affected by the installed source.

The spatial average power calibration term was determined by exciting the wall at twelve positions, and recording the input power and the velocities at ten remote positions.

7.2. Results and discussion

The mean values and the standard deviations of the power calibration term, without and with the

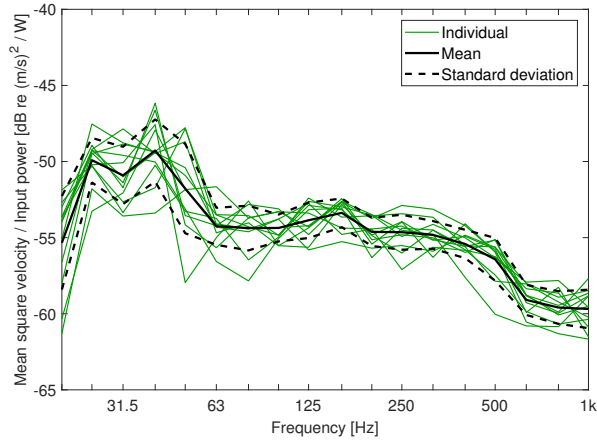


Figure 21: Case Study 3 – Source substitution method – Average power calibration term measured with an instrumented hammer. The receiver structure was excited at 12 positions, and the velocity responses were measured at 10 positions. The micro-CHP unit was not mounted on the wall during the measurements.

micro-CHP unit in place, are shown in Figures 21 and 22, respectively. In both cases, the standard deviation is approximately 1 dB above 50 Hz and up to 3 dB below 50 Hz. The mean values of the power calibration term without and with the source mounted on the wall are shown in Figure 23. The two curves agree closely, highlighting that it is possible to obtain an average power calibration term with the source in place, provided the source does not dynamically load the receiver structure.

7.3. Resulting sound pressure levels in a receiving room

To illustrate the usefulness of the procedures presented in this paper, the determined source power of the micro-CHP unit is used to predict the resulting sound pressure level in a receiving room. The prediction follows EN 15657-1 [29] and EN 12354 Part 5 [5]. The predicted sound pressure level is then compared to a criterion curve for the assessment of low-frequency noise complaints during night-time [30]. The estimated source power can thus be used as a design criterion.

The source power determined using the substitution method was used to estimate sound pressure levels in a reference building. The Standard EN 15657-1 [29] gives guidance on the calculation of a reference structure-borne sound pressure level in a receiver room diagonally below the source room (Annex C of [29]). The micro-CHP unit is assumed mounted on the reference wall and the diagonal

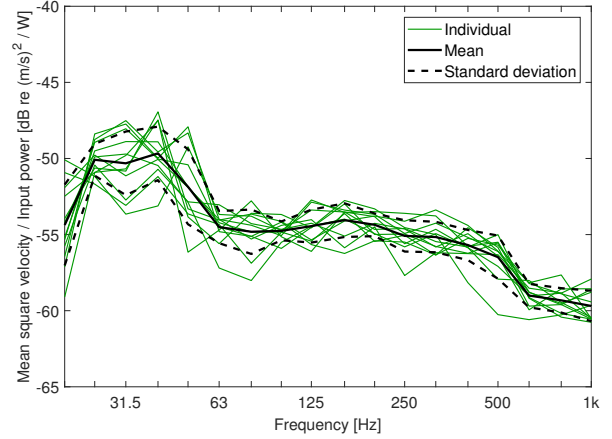


Figure 22: Case Study 3 – Source substitution method – Average power calibration term measured with an instrumented hammer. The receiver structure was excited at 12 positions, and the velocity responses were measured at 10 positions. The micro-CHP unit was mounted on the wall during the measurements.

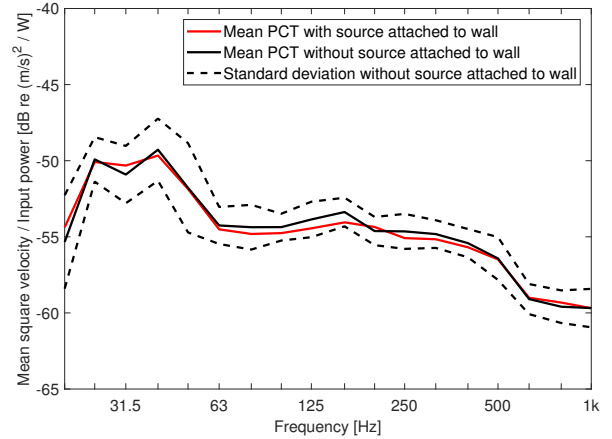


Figure 23: Case Study 3 – Source substitution method – Comparison of average power calibration terms without and with the micro-CHP unit mounted on the wall. The close agreement between the two cases indicates that the unit does not dynamically load the wall, and that the power calibration term can be determined even after installation of the unit.

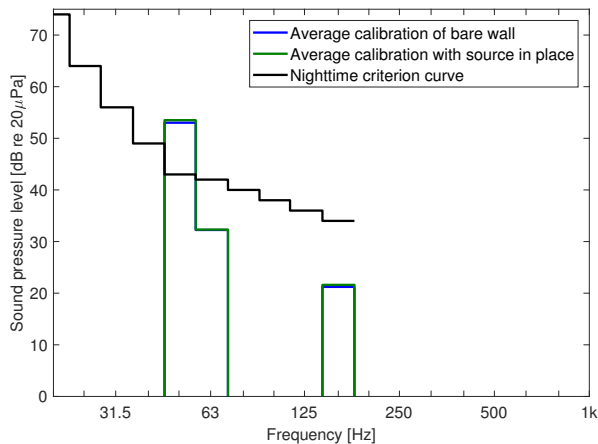


Figure 24: Case Study 3 – Reference sound pressure level in diagonally adjacent receiver room, calculated according to Annex C of EN 15657-1:2009 [29]. The nighttime criterion curve was taken from [30].

transmission (downwards) is considered. The reference wall is of 100 mm concrete block with an infinite plate mobility of $Y_\infty = 5 \times 10^6 \text{ ms}^{-1}/\text{N}$. The length of the cross-junction between floor and wall is 4 m, and the size of the source and receiver rooms are $3 \text{ m} \times 4 \text{ m} \times 2.5 \text{ m}$ and $5 \text{ m} \times 4 \text{ m} \times 2.5 \text{ m}$, respectively. The product of the resultant transmission function and the source power gives the sound pressure level in Figure 24. Also shown is the criterion curve for the assessment of low-frequency noise complaints during night-time [30].

Comparison of the predicted sound pressure levels with the criterion curve indicates that complaints are likely for the installation due to the 10 dB excess of the 50 Hz tonal component. This result is indicative rather than representative. In a real installation, pipe-borne transmission can significantly affect noise levels in the receiver room. The transmission function in Annex C of EN 15657-1 only considers the transmission to a receiver room diagonally below the source room. The unit may be mounted on a wall separating a receiver room on the same level as the source room. The transmission functions for this case can be calculated using EN 12354 Part 5 [5].

This case study demonstrates how structure-borne sound source power levels, determined by the source substitution method, can be used for assessment of noise complaints and compliance with set limits.

8. Summary and Conclusions

Three case studies were conducted to investigate the source substitution method for structure-borne sound sources. In the first study, the power injected by a simple test source into a free aluminium plate was determined using direct and indirect methods. The results for the isolated reception plate method underestimated the directly measured power by approximately 4 dB on average.

Source substitution was investigated with three calibration options: steady-state, transient, spatial average. The source power could be determined within about 1 dB on average compared with direct measurements, with maximum deviations of 4 dB. The practically most beneficial methods of using transient calibration and using an average calibration factor yielded the same accuracy.

In the second study, the power injected by a source into a concrete transmission suite floor was determined using the source substitution method. The source had been previously used in round robin (RR) tests, which provided a transmitted power for comparison. The estimated power using source substitution was determined within 6 dB of the RR results. The use of an instrumented hammer for calibration yielded similar results, as did spatial averaging.

The use of the reception plate method with a connected plate is problematical, mainly due to the loss factor determination. As a consequence, the source power was consistently under-estimated.

The third study provided an example of a practical implementation of the substitution method. A micro-CHP was operated on a masonry wall. The power calibration terms were obtained with an impulse hammer, on the wall alone and with the source in place. No significant difference was observed, indicating that the receiver wall can be calibrated with the source in place, provided the source mobility is significantly higher than the receiver mobility.

To demonstrate how the source power can be used, a reference sound pressure level in a receiver room was calculated and compared with a criterion curve for the assessment of low-frequency noise complaints.

The source substitution method is a promising development of the reception plate method. While the latter can be used if a free concrete reception plate is available, the former circumvents problems of determining the total loss factor of coupled plates

and of the average response velocity, and therefore has application to real building conditions. The use of the instrumented hammer for the calibration and the use of an average calibration factor significantly increases the practicality of the method.

Acknowledgements

The authors gratefully acknowledge the financial support provided by the Engineering and Physical Sciences Research Council of the UK under grant EP/H040293/1.

References

- [1] B. A. T. Petersson, B. M. Gibbs, Towards a structure-borne sound source characterization, *Applied Acoustics* 61 (3) (2000) 325–343.
- [2] A. T. Moorhouse, On the characteristic power of structure-borne sound sources, *Journal of Sound and Vibration* 248 (3) (2001) 441–459.
- [3] R. H. Lyon, *Statistical Energy Analysis of Dynamical Systems: Theory and Applications*, MIT Press, 1975.
- [4] R. J. M. Craik, *Sound Transmission Through Buildings: Using Statistical Energy Analysis*, Gower Publishing Ltd, 1996.
- [5] BS EN 12354: Building acoustics – Estimation of acoustic performance of buildings from the performance of elements – Part 5: Sound levels due to service equipment (2009).
- [6] BS EN ISO 3740: Acoustics – Determination of sound power levels of noise sources – Guidelines for the use of basic standards (2001).
- [7] BS EN ISO 3741: Acoustics – Determination of sound power levels of noise sources using sound pressure – Precision methods for reverberation test rooms (2010).
- [8] BS EN ISO 3743: Acoustics – Determination of sound power levels of noise sources using sound pressure – Engineering methods for small, movable sources in reverberant fields – Part 2: Methods for special reverberation test rooms (2009).
- [9] BS EN ISO 3745: Acoustics – Determination of sound power levels of noise sources using sound pressure – Precision methods for anechoic and semi-anechoic rooms (2009).
- [10] BS EN ISO 3744: Acoustics – Determination of sound power levels of noise sources using sound pressure – Engineering methods for an essentially free field over a reflecting plane (2010).
- [11] BS EN ISO 9614: Acoustics – Determination of sound power levels of noise sources using sound intensity – Part 1: Measurement at discrete points (1997).
- [12] BS EN ISO 9614: Acoustics – Determination of sound power levels of noise sources using sound intensity – Part 2: Measurement by scanning (1997).
- [13] BS EN ISO 3743: Acoustics – Determination of sound power levels of noise sources using sound pressure – Engineering methods for small, movable sources in reverberant fields – Part 1: Comparison method for a hard-walled test room (2010).
- [14] BS EN ISO 3747: Acoustics – Determination of sound power levels of noise sources using sound pressure – Engineering/survey methods for use in-situ in a reverberant environment (2010).
- [15] L. Cremer, M. Heckl, B. A. T. Petersson, *Structure-Borne Sound: Structural Vibrations and Sound Radiation at Audio Frequencies*, 3rd Edition, Springer, 2005.
- [16] C. Hopkins, *Sound Insulation*, 1st Edition, Elsevier, 2007.
- [17] R. V. Waterhouse, Interference patterns in reverberant sound fields, *The Journal of the Acoustical Society of America* 27 (2) (1955) 247–258.
- [18] A. Vogel, O. Kornadt, V. Wittstock, W. Scholl, On the measurement of sound power on reception plates, in: *Proceedings of ICSV19*, Vilnius, 2012.
- [19] A. Vogel, O. Kornadt, V. Wittstock, W. Scholl, Measurement and prediction of structure-borne sound power in plate-shaped building elements, in: *Proceedings of INTER-NOISE 2012*, New York, 2012.
- [20] M. M. Späh, B. M. Gibbs, Reception plate method for characterisation of structure-borne sound sources in buildings: Assumptions and application, *Applied Acoustics* 70 (2) (2009) 361–368.
- [21] C. Hopkins, M. Robinson, Using transient and steady-state {SEA} to assess potential errors in the measurement of structure-borne sound power input from machinery on coupled reception plates, *Applied Acoustics* 79 (0) (2014) 35 – 41.
- [22] K. Larsson, C. Simmons, Measurements of structure-borne sound from building service equipment by a substitution method – Round robin comparisons, *Noise Control Engineering Journal* 59 (1) (2011) 75–86.
- [23] Bs en 12354: Building acoustics - estimation of acoustic performance of buildings from the performance of elements - part 2: Impact sound insulation between rooms (2000).
- [24] J. Scheck, B. Gibbs, Impacted lightweight stairs as structure-borne sound sources, *Applied Acoustics* 90 (0) (2015) 9 – 20.
- [25] C. Höller, B. M. Gibbs, Inverse method to obtain blocked forces of vibrating sound sources in buildings, *Acta Acustica united with Acustica* 103 (4) (2017) 639–649.
- [26] ISO 7626: *Vibration and Shock – Experimental determination of mechanical mobility* (1986).
- [27] M. M. Späh, B. M. Gibbs, Reception plate method for characterisation of structure-borne sound sources in buildings: Installed power and sound pressure from laboratory data, *Applied Acoustics* 70 (11-12) (2009) 1431–1439.
- [28] V. Wittstock, M. Villot, J. Scheck, Results of a round robin on structure-borne sound power, in: *Proceedings of Forum Acusticum 2011*, Aalborg, 2011.
- [29] BS EN 15657: Acoustic properties of building elements and of buildings – Laboratory measurement of airborne and structure-borne sound from building equipment – Part 1: Simplified cases where the equipment mobilities are much higher than the receiver mobilities, taking whirlpool baths as an example (2009).
- [30] A. T. Moorhouse, D. C. Waddington, M. D. Adams, A procedure for the assessment of low frequency noise complaints, *The Journal of the Acoustical Society of America* 126 (3) (2009) 1131–1141.